Journal of Engineering Science *Vol. XXXII, no. 2 (2025), pp. 35 - 45*
Fascicle *Electronics and Computer Science* *ISSN 2587-3474*
Topic *Microelectronics and Nanotechnologies* *eISSN 2587-3482*

https://doi.org/10.52326/jes.utm.2025.32(2).03
UDC 539.2:543.42:621.3.049.77

IN-DEPTH PROPERTIES ANALYSIS OF $ZnAl_2O_4$/ZnO MICRO-NANOSTRUCTURES

Cristian Lupan *, ORCID: 0000-0003-2268-6181

Technical University of Moldova, 168, Stefan cel Mare Blvd., Chisinau, Republic of Moldova
* Corresponding author: Cristian Lupan, cristian.lupan@mib.utm.md

Received: 04. 08. 2025
Accepted: 05. 14. 2025

Abstract. This manuscript presents characterization of $ZnAl_2O_4$/ZnO micro-nanostructures of their morphological, chemical, structural and sensing properties. The ZnO micro-nanostructures obtained using flame transport synthesis were covered with $ZnAl_2O_4$ nanodots by chemical approach. Morphological, chemical and structural properties have been investigated using SEM, EDX and XRD, respectively. Scanning electron microscopy investigation shows the formation of micro-nanostructures of different morphologies, namely tetrapods and nanowires, covered with nanodots. The EDX study revealed the chemical composition of the micro-nanostructures, confirming the presence of Al on the micro-nanostructures' surfaces too. The XRD pattern of the studied micro-nanostructures shows the presence of ZnO and $ZnAl_2O_4$ crystalline phases in the grown material. A single $ZnAl_2O_4$/ZnO nanostructure was integrated into a device by FIB/SEM and tested to a series of gases at different operating temperatures, demonstrating selectivity to 100 ppm hydrogen gas and response value of ~1.2 up to ~3.65 at 20 °C and 150 °C, respectively. A sensing mechanism to hydrogen gas was proposed, involving free electrical charge transfer between ZnO wire and $ZnAl_2O_4$ nanodots. Based on the knowledge gained, optimization of hydrogen gas sensors using the methods and nanomaterials presented herein is envisioned.

Keywords: *nanodots, energy-dispersive X-ray spectroscopy, scanning electron microscope, Rigaku X-ray diffraction, spinel, ternary, $ZnAl_2O_4$, gas sensor.*

Rezumat. În această lucrare sunt prezentate proprietățile morfologice, chimice, structurale și senzoriale ale micro-nanostructurilor $ZnAl_2O_4$/ZnO. Micro-nanostructurile de ZnO obținute prin metoda sintezei prin transport de flacără au fost acoperite cu nanopuncte de $ZnAl_2O_4$ prin metoda chimică. Proprietățile morfologice, chimice și structurale au fost investigate utilizând SEM, EDX și XRD. Investigația prin microscopie electronică de scanare arată formarea de micro-nanostructuri de diferite morfologii, și anume tetrapozi și nanofire, acoperite cu nanopuncte. Studiul EDX a relevat compoziția chimică a micro-nanostructurilor, confirmând prezența Al și pe suprafețele micro-nanostructurilor. Difractograma XRD a micro-nanostructurilor studiate arată prezența fazelor cristaline ZnO și $ZnAl_2O_4$ în materialul obținut. Prin intermediul FIB/SEM a fost integrată o singură nanostructură $ZnAl_2O_4$/ZnO într-un dispozitiv și testată la o serie de gaze la diferite temperaturi de operare, demonstrând selectivitate la 100 ppm hidrogen cu valoarea răspunsului de ~1.2 la 20 °C până la ~3.65 la 150 °C. A fost propus un mecanism de detecție a hidrogenului, care implică transferul

sarcinilor electrice libere dintre firul de ZnO și nanopunctele de $ZnAl_2O_4$. Pe baza rezultatelor obținute, se preconizează optimizarea senzorilor de hidrogen utilizând metodele și nanomaterialele prezentate.

Cuvinte-cheie: *nanopuncte, spectroscopie cu raze X cu dispersie de energie, microscop electronic cu scanare, difracție de raze X Rigaku, spinel, ternar, $ZnAl_2O_4$, senzor de gaz.*

1. Introduction

Metal oxides (CuO, ZnO, MoO_3, In_2O_3, etc.) are a group of materials that can be used in various applications, due to their properties and various methods of synthesis [1–6]. For sensing applications, a great interest is in developing devices capable of detecting reliably and accurately a target gas in ambient conditions and mixtures of gases [2]. Pristine semiconductor metal oxides lack selectivity, high response and require high operating temperatures devices [7]. These drawbacks can be improved by fine tuning the material characteristics and performances via additives, crystalline phase control or mixing different materials [7].

ZnO can be used for diverse types of applications, due to a multitude of morphology and cost-efficient methods of obtaining [3,8]. Considering its properties (bandgap ~3.37 eV, chemical and thermal stability, high mobility of electrons, large exciton binding energy ~60 meV, etc.), zinc oxide can be used for sensing applications, such as UV and gas sensors [9-11]. Previous results showed that pure ZnO has low selectivity and high working temperatures, showing response to a wide range of VOC vapors (formaldehyde, benzene, acetone, ethanol, methanol, etc.) at 200 – 400 °C [11,12]. Different methods to improve sensing devices based on this material were reported before, including doping [10], functionalization [11,13], formation of junctions [8,9,14], and of heterostructures [15] etc.

Oxide spinel compounds (AB_2O_4) can be used for various types of applications, including gas sensing [16]. For example, Zn_2SnO_4 was used as ethanol, acetone and nitrogen dioxide sensor at operating temperatures of 200-400 °C [17]. A carbon monoxide sensor based on $ZnCo_2O_4$ was presented before, capable of detecting 300 ppm of test gas at 200 °C [18]. Lowering the working temperature of sensors is an important task in decreasing power consumption and complexity of devices [19].

$ZnAl_2O_4$ (bandgap ~3.8 eV) is a promising material for use in different applications, as catalyst, optoelectronic, etc., due to its thermal stability, electronic and chemical properties [16,20–22]. There are various methods for obtaining spinel type metal oxide nanostructures such as hydrothermal, co-precipitation, sol-gel, biological, calcination etc. [16,21-23]. Another method for synthesizing $ZnAl_2O_4$ is the solution combustion synthesis method, obtaining spherical and well crystalline particles [24]. Previous works showed the possibility of using $ZnAl_2O_4$ or ZnO/$ZnAl_2O_4$ combination as sensing material for different types of gases: hydrogen, propane, carbon monoxide, etc. [16,22,25,26].

Hydrogen is a versatile gas that can be used in various applications from automotive, material synthesis, heating, up to treatment of diseases [22,27]. Due to its explosive nature and the lack of color, odor and taste, which makes it difficult to detect by human senses, this gas poses a significant hazard during its use and storage, leading to the necessity of small, accurate and reliable devices that are capable of detecting it [28].

The main goal of this work is to present a method of obtaining $ZnAl_2O_4$/ZnO micro-nanostructures and to study in detail its properties, in order to use this material combination

as sensing material. Morphological, chemical, structural and sensing properties have been investigated in detail, with the results summarized in this paper.

2. Materials and Methods

Zinc oxide (ZnO) micro-nanostructures obtained by flame transport synthesis (FTS) method were used as base material, using Zn metal microparticles as precursor and polyvinyl butyral powder as a sacrificial polymer, with the process described in details in paper [29]. Chemical method was used to cover ZnO with zinc aluminate ($ZnAl_2O_4$), using aluminum acetate basic hydrate ($AlC_4H_7O_5 \cdot H_2O$, purity >98%) mixed with diluted ethanol (100%) in a glass container as precursors, with the process described in detail in work [16]. Ethanol was evaporated by placing the sample on a plate heated to 90 °C for 14h. At the end the nanostructures were thermally annealed on quartz substrate at 1000 °C for 3h in air.

The morphology and chemical composition of obtained micro-nanostructures was studied using scanning electron microscope (SEM) and energy-dispersive X-ray spectroscopy (EDX) using Zeiss Supra 55VP. Structural properties have been investigated using Rigaku X-ray diffraction (XRD).

In order to obtain electrical devices, a single $ZnAl_2O_4$/ZnO nanostructure was placed on a Si/SiO_2 (525 μm/800 nm) substrate with two prepatterned Cr/Au (11 nm/170 nm) electrodes and connected using focused ion beam scanning electron microscope (FIB-SEM, FEI Helios Nanolab 600) for depositing Pt contacts [30,31].

Gas sensing and electrical properties of the developed devices were investigated using two-probe approach and a Keithley 2400 source meter, controlled via LabView software [31]. Samples were tested to a series of gases with concentration of 100 ppm at different operating temperatures from room temperature (20 °C) up to 150 °C. The relative humidity was monitored and controlled at 10% during all measurements.

The gas response (S) was determined using the ratio of current in air (I_{air}) and during gas exposure (I_{gas}):

$$S = \frac{I_{gas}}{I_{air}} \quad (1)$$

3. Results and discussion

SEM was used to investigate morphological properties of obtained micro-nanostructures using FTS and chemical method, with the results presented in Figure 1. In Figure 1a and 1b are shown low and high magnification SEM images of as-grown ZnO, observing interconnected nanostructures, namely tetrapods and nanowires, with various sizes. Interconnected nanostructures or individual tetrapod/nanowire can be potentially used for sensing devices used for ultraviolet light or gas sensing [29,32].

The wrinkles visible on the ZnO surface at high magnification (Figure 1b) are due to the high temperature of 900 °C during flame transport synthesis [23]. The tetrapod arm diameters, determined from Figure 1b, is ~0.5 – 2.5 μm. Previous studies using ZnO obtained via FTS showed that the synthesis temperature has a major effect on the size and diameter of the obtained nanostructures [32].

Figure 1c represents higher magnification SEM images of $ZnAl_2O_4$/ZnO micro-nanostructures obtained using chemical method followed by 3h thermal annealing at 1000 °C, observing that micro-nanostructures have tetrapodal or nanowires morphology with various diameters and lengths. Diameter of nano-microstructures, determined from Figure 1c, is ~0.5 – 2.5 μm, which is similar to as-deposited ZnO, showing that 3h annealing at 1000 °C

has no visible effect on the size after initial deposition using FTS. The investigated tetrapods and nanowires have higher surface roughness compared to ZnO structures. Small nanodots of $ZnAl_2O_4$ are visible on the surface of deposited micro-nanostructures after thermal annealing (see Figure 1c).

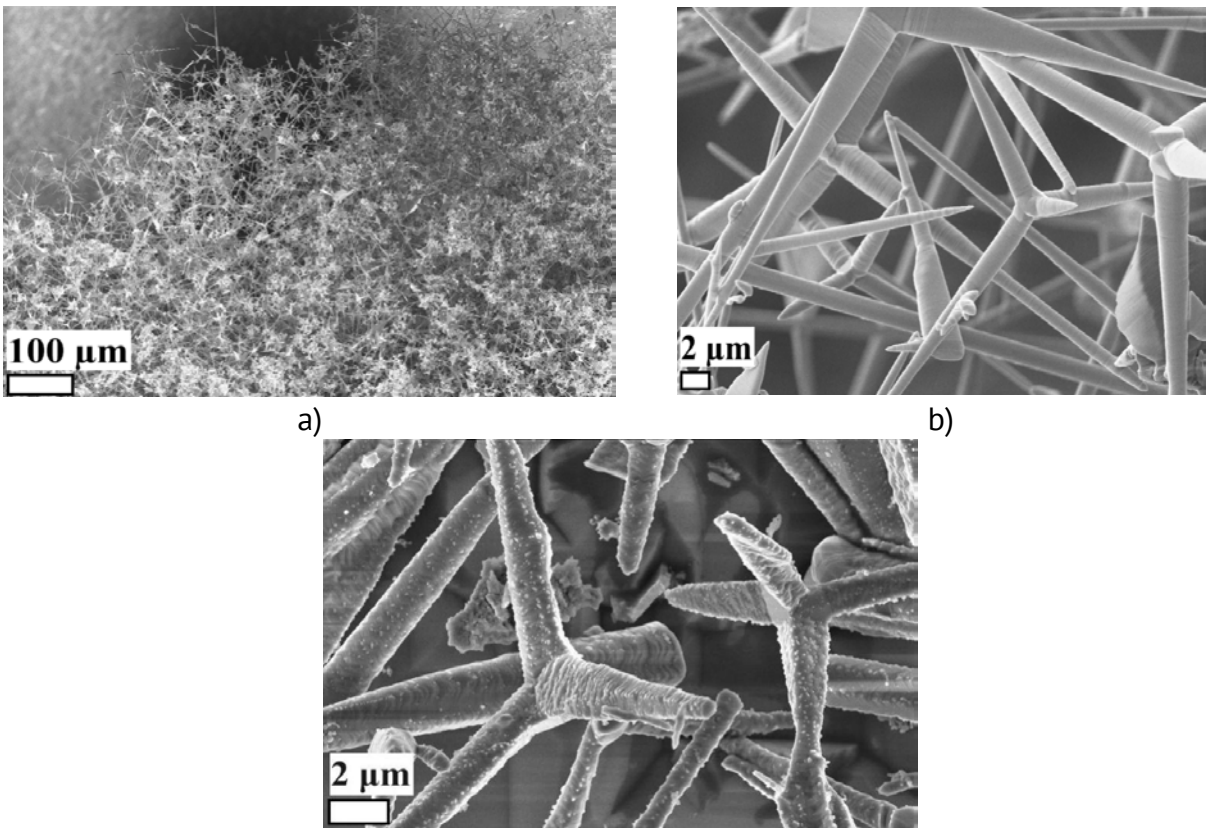

a) b)

c)

igure 1. SEM images of: a) and b) ZnO micro-nanostructures at low and high magnification; c) $ZnAl_2O_4$/ZnO micro-nanostructures annealed at 1000 °C for 3 h.

Using high-magnification SEM image and microscope software tools, the size of the deposited $ZnAl_2O_4$ nanodots was determined, as presented in Figure 2. The average nanodot size is ~65-75 nm and are spread randomly on the surface of the nanowire. The nanodots size is similar to $ZnAl_2O_4$ nanocrystals, with grain size of ~50 nm, reported in previous work [21].

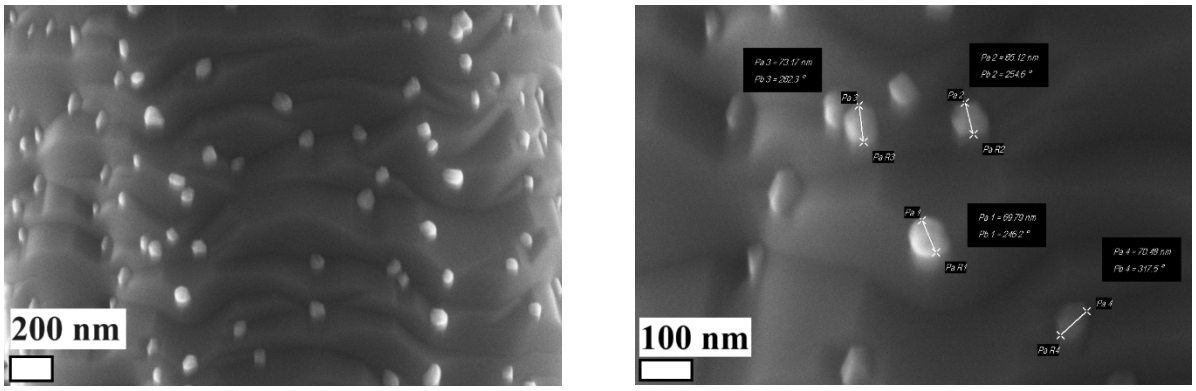

a) b)

Figure 2. SEM image of surface of $ZnAl_2O_4$/ZnO micro-nanostructures annealed at 1000 °C for 3h in air and measured at different magnifications: a) 200 nm scale bar; and b) 100 nm scale bar.

EDX mapping was used to investigate the chemical properties of grown micro-nanostructures in a target area (Figure 3a). EDX results are presented in Figure 3b-d, detecting three elements: Zn, O and Al, distributed on the surface of sample.

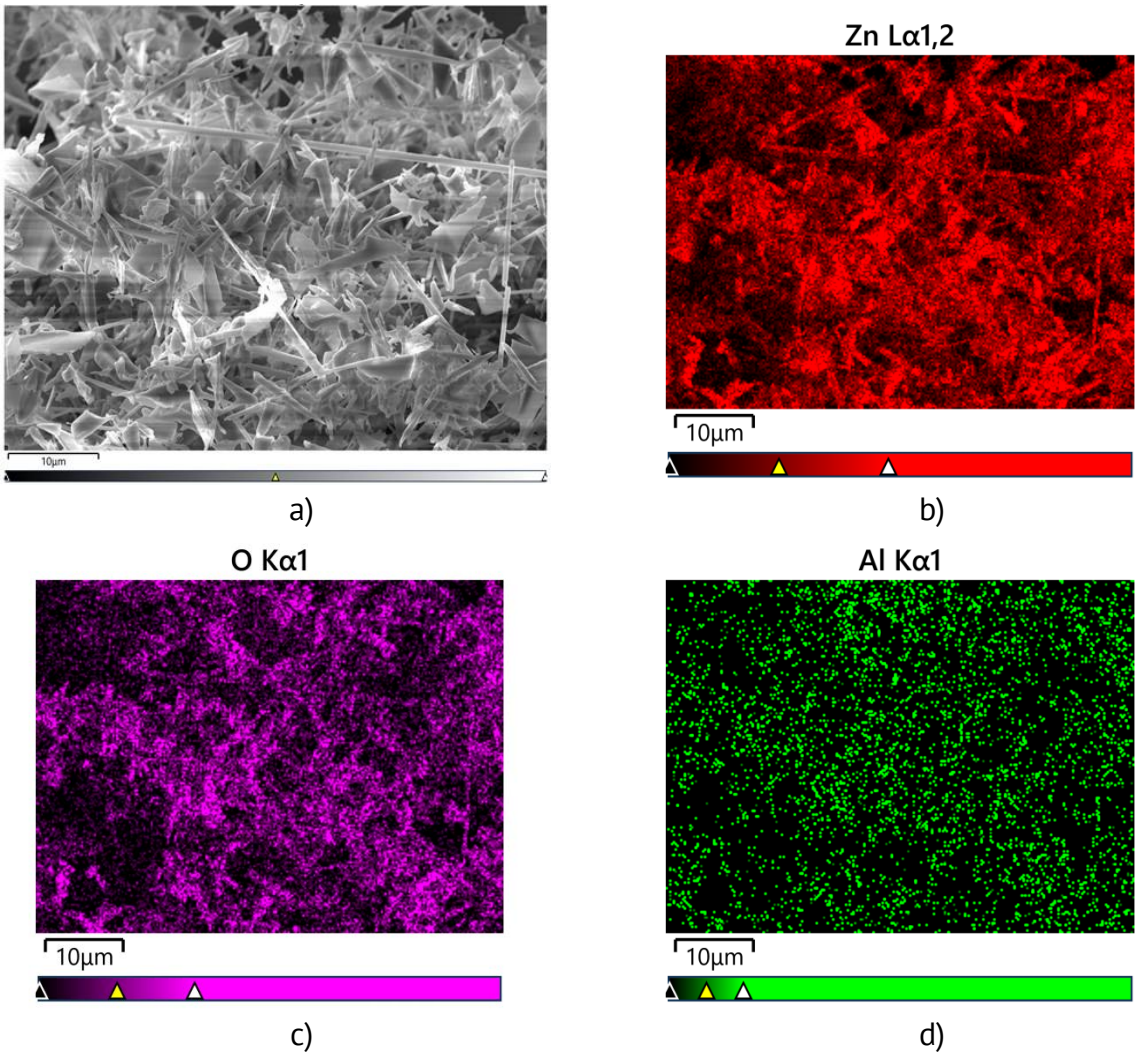

Figure 3. EDX mapping of $ZnAl_2O_4$/ZnO micro-nanostructures annealed at 1000 °C for 3h: a) scanned area; b) distribution of Zn; c) distribution of O; d) distribution of Al.

A quantitative analysis of elements in the studied $ZnAl_2O_4$/ZnO micro-nanostructures is presented in Table 1, observing smaller presence of Al (0.27 at.%), compared to Zn (50.18 at.%) and O (49.55 at.%).

Table 1

EDX results for atomic % of elements present in micro-nanostructures

Element	Atomic %
O	49.55
Al	0.27
Zn	50.18

The results for EDX scan for a single nanowire are presented in Figure 4, where Zn, O and Al elements were detected. As can be seen, Zn and O are present in the nanowire, while Al covers measured surface, due to the use of the chemical method of deposition.

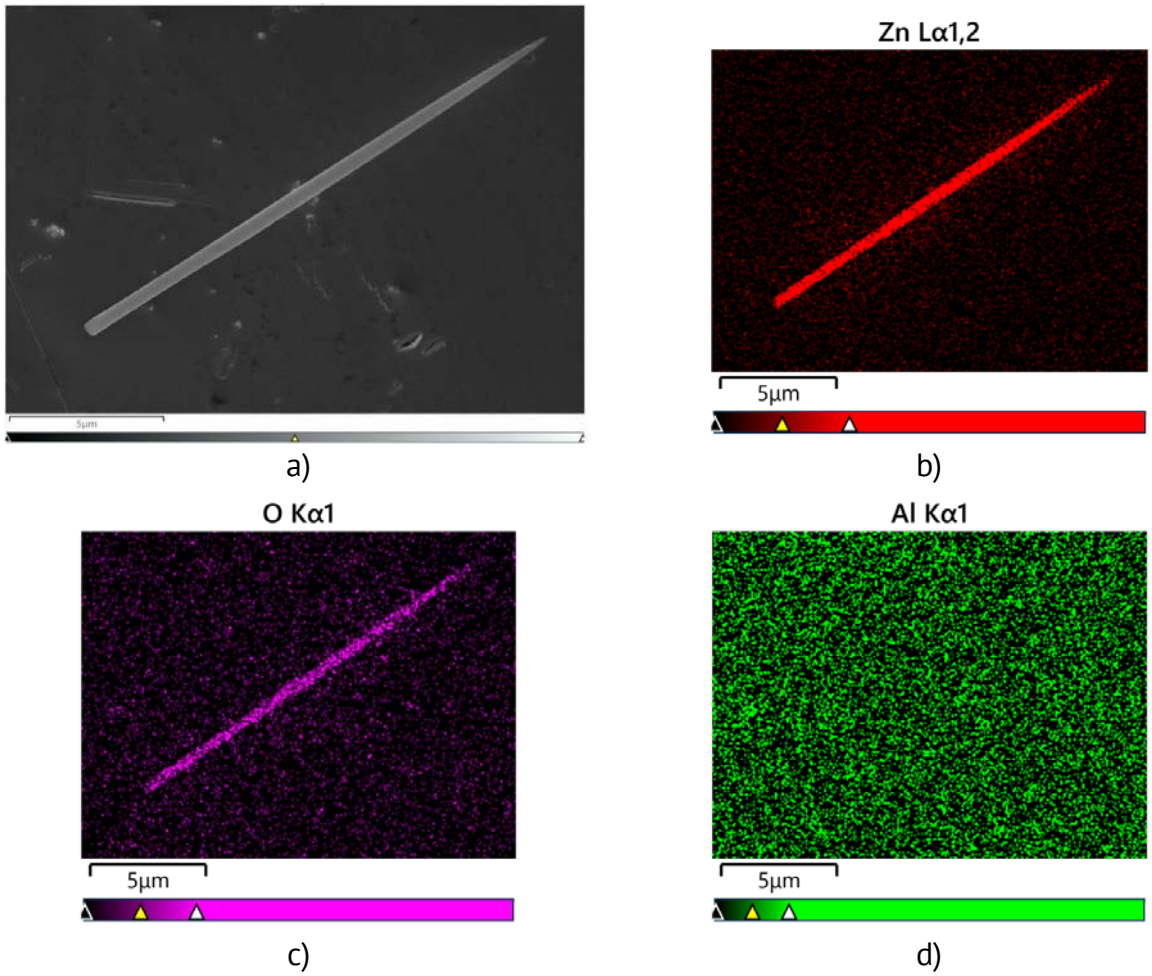

Figure 4. EDX mapping of $ZnAl_2O_4$/ZnO single nanowire annealed at 1000 °C for 3 h: a) scanned area; b) distribution of Zn; c) distribution of O; d) distribution of Al.

EDX line scan at high magnification where nanodots are visible, is presented in Figure 5. EDX line scan technique allows chemical analysis of elements in the predominance area to be seen and measured. Y-axis presenting counts of the chemical element or relative concentration in the scanned line [33].

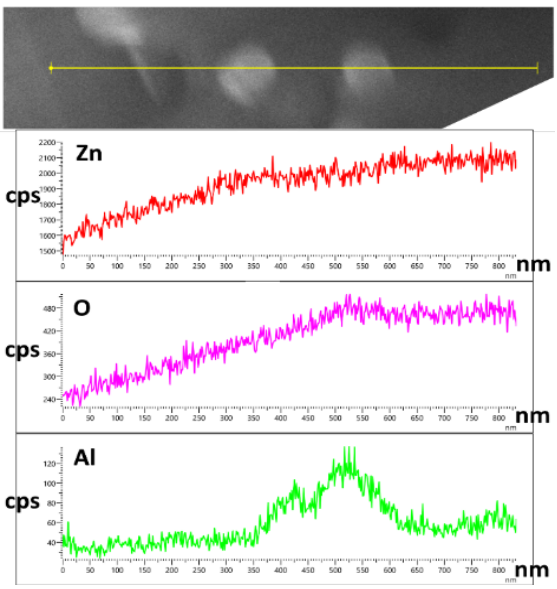

Figure 5. EDX line scan crossing nanodots of $ZnAl_2O_4$/ZnO single nanowire annealed at 1000 °C for 3h.

The presence of individual elements of Zn, Al and O is confirmed by measurement, with a low quantity of Al, as observed in investigated micro-nanostructures. Appearance of Al peak is coincident with the position of nanodots, showing presence of this element in those nanostructures, indicating that is mostly present on the newly formed nanodots.

XRD was used to confirm chemical composition, phase and structure of the obtained micro-nanostructures. The results for the XRD measurement in the 60-80° 2θ values are presented in Figure 6. Detected XRD reflections were attributed according to standard cards PDF #031161 ($ZnAl_2O_4$) and PDF #0361451 (ZnO).

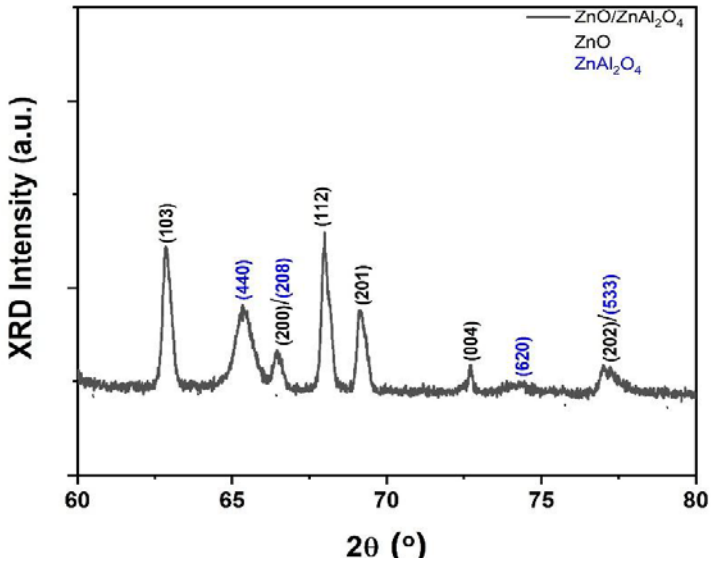

Figure 6. XRD pattern of $ZnAl_2O_4$/ZnO micro-nanostructures annealed at 1000 °C for 3h in air.

Multiple ZnO and $ZnAl_2O_4$ diffractions peaks were attributed in this range, with highest intensity for (103) and (112) ZnO planes. The highest intensity for $ZnAl_2O_4$ peak was observed for (440) plane. Some overlapping ZnO and $ZnAl_2O_4$ peaks were detected. No diffraction peaks corresponding to other materials were detected in the investigated samples.

Average crystallite size (*D*) for $ZnAl_2O_4$ (440) plane was determined using the Scherrer formula [34]:

$$D = \frac{k \cdot \lambda}{\beta \cdot cos\theta} \quad (2)$$

where: *k* – shape factor (*k* = 0.9), *λ* – wavelength of the radiation (*λ* = 1.5406 Å), *β* – full-width half maximum intensity of the reflection.

The calculated *D* is ~70.65 nm, which is similar to the measured $ZnAl_2O_4$ nanodot size from the SEM images. The sensing device based on a single $ZnAl_2O_4$/ZnO nanostructure was tested to a series of gases with concentration of 100 ppm (acetone, n-butanol, methane, ethanol, hydrogen, ammonia and 2-propanol) at different operating temperatures from 20 °C up to 150 °C, with the results presented in Figure 7.

As can be seen, response was observed only for 100 ppm hydrogen gas at all operating temperatures, meaning that sensor is selective to this gas. Response value (*S*) increased from ~1.2 up to ~3.65 with the rise of operating temperature from 20 °C to 150 °C, respectively.

Gas response and selectivity to hydrogen for $ZnAl_2O_4$/ZnO based device can be attributed to the formation of *n-n* heterostructure and use of Pt contacts for the nanostructure, which can act as catalysts too [16,22]. Increased response at 100-150 °C compared to room temperature, can be attributed to the presence of more reactive oxygen species (O^-) on the surface of the material [22].

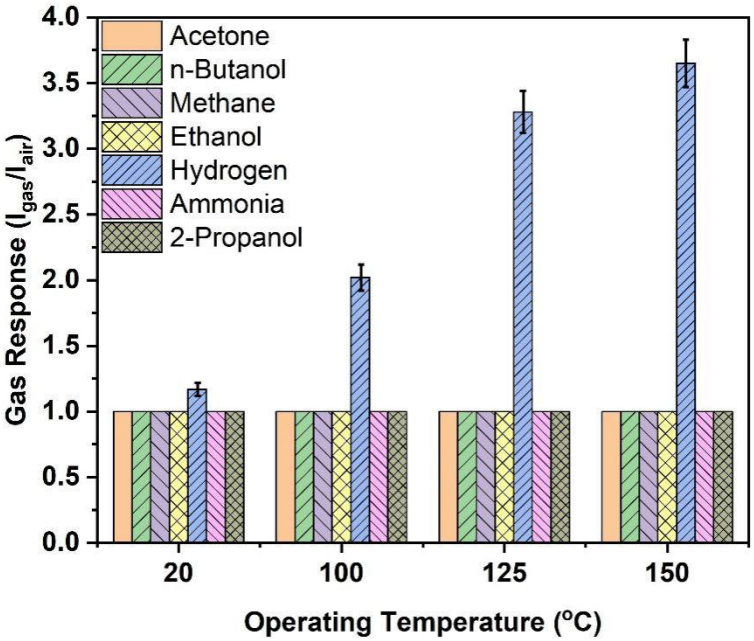

Figure 7. Gas response to a series of gases with concentration of 100 ppm at different operating temperatures for device based on a single $ZnAl_2O_4$/ZnO nanostructure annealed at 1000 °C for 3 h in air.

In Figure 8 is presented schematic representation of proposed hydrogen gas sensing mechanism for $ZnAl_2O_4$/ZnO based device. When the device is in air atmosphere (Figure 8a), oxygen species are adsorbed on the surface of the material, in this case O^- at 100-150 °C [35,36]. An electron flow between $ZnAl_2O_4$ nanodots and ZnO takes place, leading to higher concentration of free-electrons in conduction band of ZnO, which in turn increases oxygen coverage in air environment [16,37].

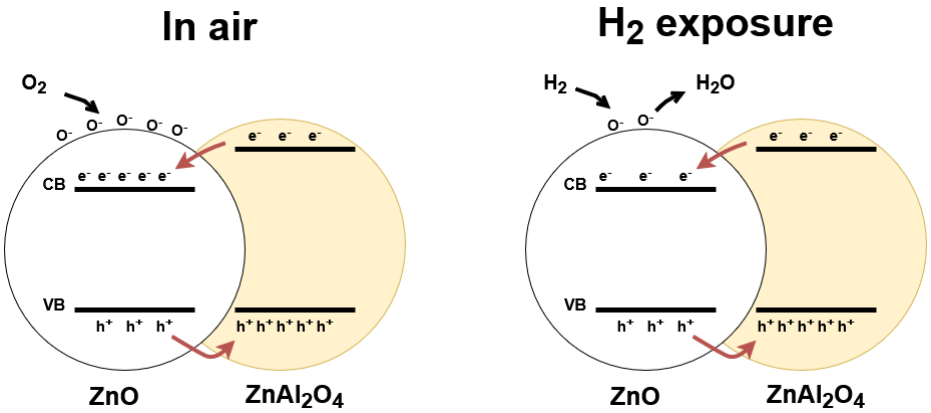

Figure 8. Schematic representation for proposed sensing mechanism for device based on single ZnO/$ZnAl_2O_4$ nanostructure: a) in air and b) during H_2 exposure.

The following reaction during hydrogen exposure takes place with the oxygen species on the surface (Figure 8b) [37]:

$$H_2 + O^- \rightarrow H_2O + e^- \quad (3)$$

The reaction leads to the release of H_2O in the environment and the captured electrons to the conduction band, increasing current. Faster oxidizing processes and increased response during hydrogen gas exposure are possible due to the free charge transfer from $ZnAl_2O_4$ to

ZnO, which was also previously reported by other authors when adding different nanoparticles on the surface of the base material [16,38].

5. Conclusions

ZnO micro-nanostructures obtained using flame transport synthesis were covered with $ZnAl_2O_4$ nanodots using chemical method, followed by annealing at 1000 °C for 3h in air. Morphological investigation shows the formation of tetrapods and nanowires, covered with small nanodots with ~65-75 nm diameter.

EDX study presented chemical composition of the sample, confirming the presence of Al, with at.% of ~0.27%. By comparing EDX results from multiple interconnected micro-nanostructures and single nanowire, it was detected that Al covers entire surface of the sample, while Zn and O is mostly present in the nanowire/tetrapod. EDX line scan indicate that appearance of Al peak is coincident with the position of nanodots, showing its presence on the newly formed nanodots.

The XRD pattern of the investigated micro-nanostructures shows presence of ZnO and $ZnAl_2O_4$ in the sample, by attributing peaks according to PDF cards of the materials.

Sensing study presented insights on the behavior of the $ZnAl_2O_4$/ZnO based device to a series of test gases at different operating temperatures, observing selectivity to 100 ppm hydrogen and a response value of ~1.2 up to ~3.65 at operating temperatures of 20 °C and 150 °C, respectively. A sensing mechanism was proposed, based on the free charge transfer between ZnO and $ZnAl_2O_4$.

The results obtained and presented in this study can be used for further enhancement of hydrogen gas sensing properties of devices based on this material, which can be potentially integrated and used in personal, industrial, environmental monitoring devices.

The results were presented and discussed at the 13th International Conference on Electronics, Communications and Computing (IC ECCO 2024), Chisinau, Republic of Moldova, 17-18 October, 2024.

Acknowledgments: This paper was supported by project code 24.80012.5007.15TC by National Agency for Research and Development of Moldova at Technical University of Moldova.

Cristian Lupan gratefully acknowledges: Kiel University, Germany, Department of Materials Science, Chair for Multicomponent Materials and Chair of Functional Nanomaterials; PSL Université, Chimie-ParisTech IRCP, Paris, France; Twente University, Enschede, the Netherlands for collaboration in 2023 – 2025 and Technical University of Moldova for constant support. C. Lupan would like to express special appreciation and thanks to Ph.D. scientific adviser Professor, dr. hab. Artur Buzdugan (TUM) and assoc. prof. dr. Nicolai Ababii (TUM) for their support, comments and discussions on this work.

Conflicts of Interest: The author declares no conflict of interest.

References

1. Wang, C.; Yin, L.; Zhang, L.; Xiang, D.; Gao, R. Metal oxide gas sensors: Sensitivity and influencing factors. *Sensors* 2010, 10, pp. 2088–2106.
2. Schröder, S.; Ababii, N.; Brînză, M.; Magariu, N.; Zimoch, L.; Bodduluri, M. T.; Strunskus, T.; Adelung, R.; Faupel, F.; Lupan, O. Tuning the Selectivity of Metal Oxide Gas Sensors with Vapor Phase Deposited Ultrathin Polymer Thin Films. *Polymers* (Basel) 2023, 15, 524.
3. Mishra, Y. K.; Kaps, S.; Schuchardt, A.; Paulowicz, I.; Jin, X.; Gedamu, D.; Wille, S.; Lupan, O.; Adelung, R. Versatile fabrication of complex shaped metal oxide nano-microstructures and their interconnected

networks for multifunctional applications. *KONA Powder Part J* 2014, 31, pp. 92–110.
4. Paulowicz, I.; Postica, V.; Lupan, O.; Wolff, N.; Shree, S.; Cojocaru, A.; Deng, M.; Mishra, Y. K.; Tiginyanu, I.; Kienle, L.; Adelung, R. Zinc oxide nanotetrapods with four different arm morphologies for versatile nanosensors. *Sensors Actuators, B Chem* 2018, 262, pp. 425–435.
5. Lupan, O.; Chow, L.; Chai, G.; Heinrich, H.; Park, S.; Schulte, A. Growth of tetragonal SnO_2 microcubes and their characterization. *J Cryst Growth* 2008, 311, pp. 152–155.
6. Khallaf, H.; Chen, C. T.; Chang, L. B.; Lupan, O.; Dutta, A.; Heinrich, H.; Haque, F.; Del Barco, E.; Chow, L. Chemical bath deposition of SnO_2 and Cd_2SnO_4 thin films. *Appl Surf Sci* 2012, 258, pp. 6069–6074.
7. Degler, D.; Weimar, U.; Barsan, N. Current Understanding of the Fundamental Mechanisms of Doped and Loaded Semiconducting Metal-Oxide-Based Gas Sensing Materials. *ACS Sensors* 2019, 4, pp. 2228–2249.
8. Newton, M. C.; Shaikhaidarov, R. ZnO tetrapod p-n junction diodes. *Appl Phys Lett* 2009, 94, pp. 20–23.
9. Khan, R.; Ra, H. W.; Kim, J. T.; Jang, W. S.; Sharma, D.; Im, Y. H. Nanojunction effects in multiple ZnO nanowire gas sensor. *Sensors Actuators, B Chem* 2010, 150, pp. 389–393.
10. Lupan, C.; Khaledialidusti, R.; Mishra, A. K.; Postica, V.; Terasa, M. I.; Magariu, N.; Pauporté, T.; Viana, B.; Drewes, J.; Vahl, A.; Faupel, F.; Adelung, R. Pd-Functionalized ZnO:Eu Columnar Films for Room-Temperature Hydrogen Gas Sensing: A Combined Experimental and Computational Approach. *ACS Appl Mater Interfaces* 2020, 12, pp. 24951–24964.
11. Chai, G. Y.; Lupan, O.; Rusu, E. V.; Stratan, G. I.; Ursaki, V. V.; Sontea, V.; Khallaf, H.; Chow, L. Functionalized individual ZnO microwire for natural gas detection. *Sensors Actuators, A Phys* 2012, 176, pp. 64–71.
12. Teimoori, F.; Khojier, K.; Dehnavi, N. Z. Investigation of sensitivity and selectivity of ZnO thin film to volatile organic compounds. *J Theor Appl Phys* 2017, 11, pp. 157–163.
13. Lupan, O.; Postica, V.; Hoppe, M.; Wolff, N.; Polonskyi, O.; Pauporté, T.; Viana, B.; Majérus, O.; Kienle, L.; Faupel, F.; Adelung, R. PdO/PdO_2 functionalized ZnO:Pd films for lower operating temperature H_2 gas sensing. *Nanoscale* 2018, 10, pp. 14107–14127.
14. Kumar, V.; Rawal, I.; Kumar, V. Fabrication of n-ZnO/p-Si++ Hetero-junction Devices for Hydrogen Detection: Effect of Annealing Temperature. *Silicon* 2022, 14, pp. 7711–7723.
15. Kaur, N.; Zappa, D.; Ferroni, M.; Poli, N.; Campanini, M.; Negrea, R.; Comini, E. Branch-like NiO/ZnO heterostructures for VOC sensing. S*ensors Actuators, B Chem* 2018, 262, pp. 477–485.
16. Hoppe, M.; Lupan, O.; Postica, V.; Wolff, N.; Duppel, V.; Kienle, L.; Tiginyanu, I.; Adelung, R. $ZnAl_2O_4$-Functionalized Zinc Oxide Microstructures for Highly Selective Hydrogen Gas Sensing Applications. *Phys Status Solidi Appl Mater Sci* 2018, 215, pp. 1–13.
17. Hemmatzadeh Saeedabad, S.; Baratto, C.; Rigoni, F.; Rozati, S. M.; Sberveglieri, G.; Vojisavljevic, K.; Malic, B. Gas sensing applications of the inverse spinel zinc tin oxide. *Mater Sci Semicond Process* 2017, 71, pp. 461–469.
18. Morán-Lázaro, J. P.; López-Urías, F.; Muñoz-Sandoval, E.; Blanco-Alonso, O.; Sanchez-Tizapa, M.; Carreon-Alvarez, A.; Guillén-Bonilla, H.; Olvera-Amador, M. de la L.; Guillén-Bonilla, A.; Rodríguez-Betancourtt, V. M. Synthesis, characterization, and sensor applications of spinel $ZnCo_2O_4$ nanoparticles. *Sensors* (Switzerland) 2016, 16, 2162.
19. Lupan, O.; Postica, V.; Labat, F.; Ciofini, I.; Pauporté, T.; Adelung, R. Ultra-sensitive and selective hydrogen nanosensor with fast response at room temperature based on a single Pd/ZnO nanowire. *Sensors Actuators, B Chem* 2018, 254, pp. 1259–1270.
20. Zhang, D.; Du, C.; Chen, J.; Shi, Q.; Wang, Q.; Li, S.; Wang, W.; Yan, X.; Fan, Q. Improvement of structural and optical properties of $ZnAl_2O_4:Cr^{3+}$ ceramics with surface modification by using various concentrations of zinc acetate. *J Sol-Gel Sci Technol* 2018, 88, pp. 422–429.
21. Padmapriya, G.; Amudhavalli, M. Synthesis and characterization studies of spinel $ZnAl_2O_4$ nanoparticles prepared by Aloe vera plant extracted combustion method. *Malaya Journal of Matematik* 2020, 2, pp. 2089–2091.
22. Lupan, C.; Kohlmann, N.; Petersen, D.; Teja, M.; Buzdugan, A.; Jetter, J.; Quandt, E.; Kienle, L.; Adelung, R. Hydrogen nanosensors based on core/shell ZnO/Al_2O_3 and $ZnO/ZnAl_2O_4$ single nanowires. *Mater Today Nano* 2025, 29, 100596.
23. Rodrigues, J.; Hoppe, M.; Ben Sedrine, N.; Wolff, N.; Duppel, V.; Kienle, L.; Adelung, R.; Mishra, Y. K.; Correia, M. R.; Monteiro, T. $ZnAl_2O_4$ decorated Al-doped ZnO tetrapodal 3D networks: microstructure, Raman and detailed temperature dependent photoluminescence analysis. *Nanoscale Adv* 2020, 2, pp. 2114-2126.
24. Mirbagheri, S. A.; Masoudpanah, S. M.; Alamolhoda, S. Structural and optical properties of $ZnAl_2O_4$ powders synthesized by solution combustion method: Effects of mixture of fuels. *Optik* (Stuttg) 2020, 204, 164170.
25. Huízar-Padilla, E.; Guillén-Bonilla, H.; Guillén-Bonilla, A.; Rodríguez-Betancourtt, V. M.; Sánchez-Martínez, A.; Guillen-Bonilla, J. T.; Gildo-Ortiz, L.; Reyes-Gómez, J. Synthesis of $ZnAl_2O_4$ and evaluation of the response in

propane atmospheres of pellets and thick films manufactured with powders of the oxide. *Sensors* 2021, 21, 2362.
26. Iaiche, S.; Djelloul, A. ZnO/$ZnAl_2O_4$ nanocomposite films studied by X-Ray diffraction, FTIR, and X-Ray photoelectron spectroscopy. *J Spectrosc* 2015, 836859.
27. Zhai, X.; Chen, X.; Ohta, S.; Sun, X. Review and prospect of the biomedical effects of hydrogen. *Med Gas Res* 2014, 4, pp. 19–22.
28. Gu, H.; Wang, Z.; Hu, Y. Hydrogen gas sensors based on semiconductor oxide nanostructures. *Sensors* 2012, 12, pp. 5517-5550.
29. Mishra, Y. K.; Modi, G.; Cretu, V.; Postica, V.; Lupan, O.; Reimer, T.; Paulowicz, I.; Hrkac, V.; Benecke, W.; Kienle, L.; Adelung, R. Direct Growth of Freestanding ZnO Tetrapod Networks for Multifunctional Applications in Photocatalysis, UV Photodetection, and Gas Sensing. *ACS Appl Mater Interfaces* 2015, 7, pp. 14303–14316.
30. Lupan, O.; Chai, G.; Chow, L. Fabrication of ZnO nanorod-based hydrogen gas nanosensor. *Microelectronics J* 2007, 38, pp. 1211–1216.
31. Lupan, O.; Magariu, N.; Khaledialidusti, R.; Mishra, A. K.; Hansen, S.; Krüger, H.; Postica, V.; Heinrich, H.; Viana, B.; Ono, L. K.; Cuenya, B. R.; Chow, L.; Adelung, R.; Pauporté, T. Comparison of Thermal Annealing versus Hydrothermal Treatment Effects on the Detection Performances of ZnO Nanowires. *ACS Appl Mater Interfaces* 2021, 13, pp. 10537–10552.
32. Shree, S.; Postica, V.; Voß, L.; Lupan, C.; Mishra, Y. K.; Kienle, L.; Adelung, R.; Lupan, O. Optimization of T-ZnO Process for Gas and UV Sensors. *ACS Appl Electron Mater* 2025, 7, pp. 3848–3863.
33. Mijangos, F.; Celaya, M. A.; Gainza, F. J.; Imaz, A.; Arana, E. SEM–EDX linear scanning: a new tool for morpho-compositional analysis of growth bands in urinary stones. *J Biol Inorg Chem* 2020, 25, pp. 705–715.
34. Khorsand Zak, A.; Abd. Majid, W. H.; Abrishami, M. E.; Yousefi, R. X-ray analysis of ZnO nanoparticles by Williamson-Hall and size-strain plot methods. *Solid State Sci* 2011, 13, pp. 251–256.
35. Yamazoe, N.; Fuchigami, J.; Kishikawa, M.; Seiyama, T. Interactions of tin oxide surface with O_2, H_2O and H_2. *Surf Sci* 1979, 86, pp. 335–344.
36. Chang, S. C. Oxygen Chemisorption on Tin Oxide: Correlation Between Electrical Conductivity and Epr Measurements. *J Vac Sci Technol* 1979, 17, pp. 366–369.
37. Barsan, N.; Rebholz, J.; Weimar, U. Conduction mechanism switch for SnO_2 based sensors during operation in application relevant conditions; Implications for modeling of sensing. *Sensors Actuators, B Chem* 2015, 207, pp. 455–459.
38. Kim, H. J.; Jeong, H. M.; Kim, T. H.; Chung, J. H.; Kang, Y. C.; Lee, J. H. Enhanced ethanol sensing characteristics of In_2O_3-decorated NiO hollow nanostructures via modulation of hole accumulation layers. *ACS Appl Mater Interfaces* 2014, 6, pp. 18197–18204.

Citation: Lupan, C. In-depth properties analysis of $ZnAl_2O_4$/ZnO micro-nanostructures. *Journal of Engineering Science*. 2025, XXXII (2), pp. 35-45. https://doi.org/10.52326/jes.utm.2025.32(2).03.

Submission of manuscripts: jes@meridian.utm.md